Journal of Physics: Conference Series

PAPER • **OPEN ACCESS**

Quantifying the effect of rock armour scour protection on eigenfrequencies of a monopile supported OHVS

To cite this article: K. Winkler *et al* 2023 *J. Phys.: Conf. Ser.* **2626** 012039

Quantifying the effect of rock armour scour protection on eigenfrequencies of a monopile supported OHVS

Winkler K.[1], Weil M.[1], Sastre Jurado C.[1,2], Stuyts B.[2], Weijtjens W.[1], Devriendt C.[1]

[1] Vrije Universiteit Brussel, OWI-lab, Pleinlaan 2, 1050 Brussels, Belgium
[2] UGent, Geotechnical Laboratory, Technologiepark 68, 9052 Zwijnaarde, Belgium

E-mail: `kristof.winkler@vub.be`

Abstract. It is common practice to install scour protection systems during the construction of offshore wind farms. This is because the guidelines allow for a more optimal structural design, as the potential effects of scouring may be ignored. However, multiple sources, as well as measurements, suggest that there is an additional gain in stiffness which is not being taken into account by current guidelines. Scour protection has the ability to provide extra foundational stiffness to the monopile, which results in higher natural eigenfrequencies and mode shapes. In this paper the focus will be on an offshore high voltage station (OHVS) located in the North Sea and the impact of a rubble riprap scour protection on the foundational stiffness of the structure. Furthermore, a proposal is made on how to take these effects into account when calculating for design. This site was equipped with a mobile measurement system containing a multi-axial accelerometer, which was active in a period both before and after installation of the scour protection rock armour layer. In case of similar environmental circumstances, the eigenfrequencies of the OHVS were noticeably higher after the scour protection was installed, thus substantiating the claim of increased foundational stiffness. To perform numerical studies on the impact of the scour protection system on structural dynamics, an OHVS support structure finite element model was built. As no formally agreed upon formulation to include scour protection exists, two possible methods are proposed. One is adding a global accretion layer to model the scour protection as an additional soil layer. The other calculates an overburden pressure due to the scour protection weight, which translates to the stiffening of the upper soil layers of the foundation. Both methods have their own strengths and weaknesses, but more research on different locations and offshore structures is needed to formalize the definitive description for modelling scour protection.

1. Introduction

Since its inception, offshore wind has had some issues when comparing as designed with in situ measured properties. Despite all research efforts of the past 20 years, this mismatch still partially persists to this day. Especially the rapid expansion of the industry and the constant need for bigger and bigger turbines lead to oversized monopile (MP) supported structures. These foundations have some unknown behaviours as there is no previous practical experience to draw from. As such, many aspects of their design and maintenance still motivate a lot of research today.

Past observations suggest that one of the possible sources of current mismatch might be the impact of scour protection on the structural dynamics of offshore wind turbines (OWT). The current industry practice is to install rock armour, also called riprap, scour protection (SP) following the guidelines DNV-ST-0126. This allows to make structures that do not have to take scouring into account for their safety margins, which leads to a leaner design. However, in addition of the regular protection, this rock layer also seems to have other beneficial properties. For example, [1] states that unpublished results indicate that scour protection has a significant effect on the first natural eigenfrequencies of an OWT. It concluded that first order frequencies would increase by 1.4% for a scour protection of 1m thickness. Another publication, looking at Horns Rev [2], found that it needed to include a model for scour protection to explain its measured bending moment response. Small-scale laboratory tests and numerical simulations [3, 4] were also used to investigate the additional effects of scour protection. Both times the result of the lab test was an increased stiffness of the soil lateral response curves after scour protection installation. Recently, attempts to incorporate scour protection contribution in numerical models were bench-marked against full-scale measurements from monitored OWTs in [5, 6], concluding that simulations agree better with measurements if the scour protection system is considered in the model.

In this paper, a measurement campaign of a monopile supported Offshore high voltage station (OHVS) located in the Belgian North Sea is presented. More specifically, the structure's eigenfrequencies, derived from vibration measurements, both before and after installation of the final armour layer of the scour protection. Also, an integrated finite element (FE) model is used to investigate how to include the SP contribution to better explain the measurements.

2. Measurement campaign

2.1. Monitoring setup

A measurement campaign was conducted to obtain vibration measurements from a monopile-supported OHVS using a semi-permanent monitoring system comprising of a tri-axial accelerometer. The accelerometer was placed on the topside structure of the OHVS and returned acceleration data sampled at 100Hz. The campaign started around the winter of 2016, one month before the installation of the top layer of the scour protection, and ended a few months thereafter in the spring of 2017.

2.2. Monitored eigenfrequencies

The Power Spectral Density (PSD) of 10-minute acceleration signals is shown in Figure 1. The key frequencies of interest are highlighted. The first fore-aft (FA) and side-side (SS) modes, which are referred to as SS1 and FA1, are identified as the peaks in the PSD with the highest energy. The torsional mode is characterised by a zero-content in the vertical direction.

To determine and track these eigenfrequencies over time the automated Operational Modal Analysis (OMA) algorithm as proposed in [7] was used. The automated OMA calculates the modes using the Linear Square Complex Frequency Estimator (LSCF) algorithm on 10 minutes of data with a model order of 48 and window length of 24 [8]. This is done for both the SS and FA directions. After the modes are estimated for all the measurement data, the physical modes are identified and tracked in an unsupervised manner using the DBSCAN clustering algorithm [9]. All the modes identified in the PSD of Figure 1 (left) can be tracked with the exception of FA2. This frequency had a spread out peak in its PSD during the time frame before armour layer installation. After the scour protection was completed this issue resolved itself and FA2 could be tracked properly. The cause of this identification issue is unknown but could be the result from the measurement unit being located to close to the node of the FA2 mode. The resulting tracking of the modes is shown in Figure 1 (right) for the SS direction.

The impact of the scour protection was examined for all monitored frequencies by comparing

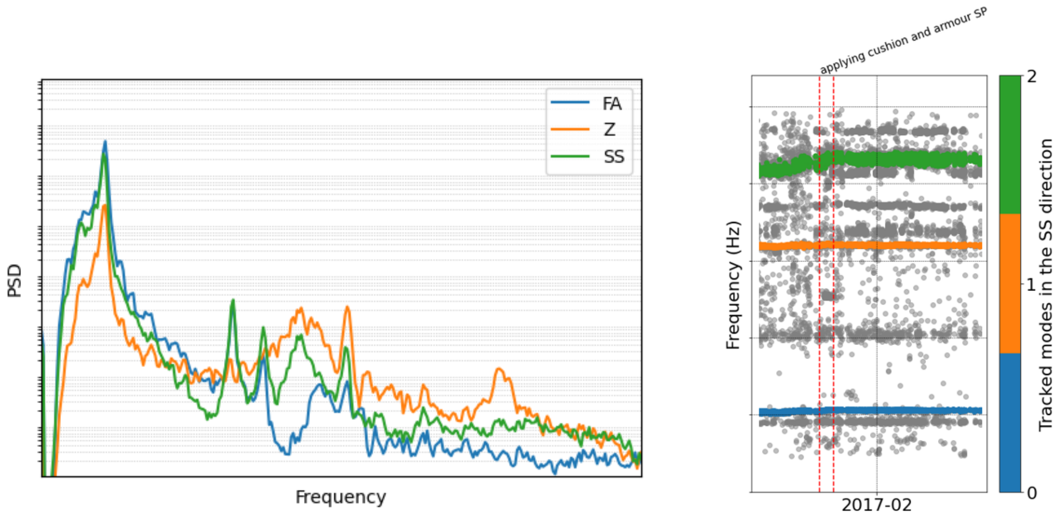

Figure 1. (left) Power Spectral Density of a 10-minute signal after the installation of the additional rock armour layer. (right) Tracking of the modes in the Side-Side (SS) direction for the whole measurement campaign, zoomed in on the period just before and after applying the rock armour layer of the scour protection. First order (blue), torsional (orange) and second order (green) modes are identified.

results before and after the installation of the rock armour. For the torsional mode, no major change in frequency is observed which suggests that the scour protection does not impact torsional stiffness significantly. However, taking environmental conditions into account, the other tracked modes show an overall increase in eigenfrequency, which could indicate a stiffer foundation response. For instance in Figure 2 the SS1 mode is shown in more detail for the full monitoring period. During the installation of the SP (in brown) an upward trend in frequency can be observed, suggesting a stiffening of the structure. Additionally, a less pronounced downward trend is observed in the first few days after the SP is installed (pink) presumably as the scour protection is settling. Comparing the SS1 frequency before (green) and (blue) the SP installation suggests a significant increase. However, one does observe a strong variability in the measured frequencies before and and after installing the SP. Eigenfrequencies of OWTs and OHVS are known to be prone to Environmental and Operational Variability (EOV). To ensure the difference in frequency before and after the installation is not due to EOV, a simple linear regression model ($f_p(\mathbf{x}) = \sum_{i=0} \beta_i x_i + f_0$) is fitted to the measurement data f_m to predict the eigenfrequencies f_p based on the environmental parameters $\mathbf{x}$[10]. In a final step the residual $f_r = f_m - f_p(\mathbf{x})$ is calculated by subtracting the model from the measurements. This residual should no longer be affected by the EOV.

The environmental data is gathered from the Meetnet Vlaamse Banken, an online database containing weather data of the North Sea provided by the Flemish government[1]. The regression model uses inputs known to influence the eigenfrequencies; wave height, sea water temperature and tidal level. A section of the data from the post SP-installation time frame $f_{m,afterSP}$ is chosen as training data as more data is available for this phase. The model is then used to predict the eigenfrequencies over the whole measuring campaign, results are shown in orange in Figure 2. The model matches the data well for the period after the stabilization of the SP (blue), resulting in a zero-mean residual f_r. Prior to the SP application, the model also follows

[1] https://meetnetvlaamsebanken.be/

most variations which are mainly related to changes in the wave height, but cannot explain the nominally lower value of the resonance frequency. A bias between the model predictions and measured frequencies appears, this bias suggests that the observed difference in eigenfrequency before and after SP cannot be explained by EOV alone. As the change in frequency coincides with the time of installation of the SP and there are no other known influence factors we conclude that the change in frequency is due to a physical change in the structure itself, in this case the completion of the SP.

Aside from the model to predict SS1 frequencies, two additional models are trained to also

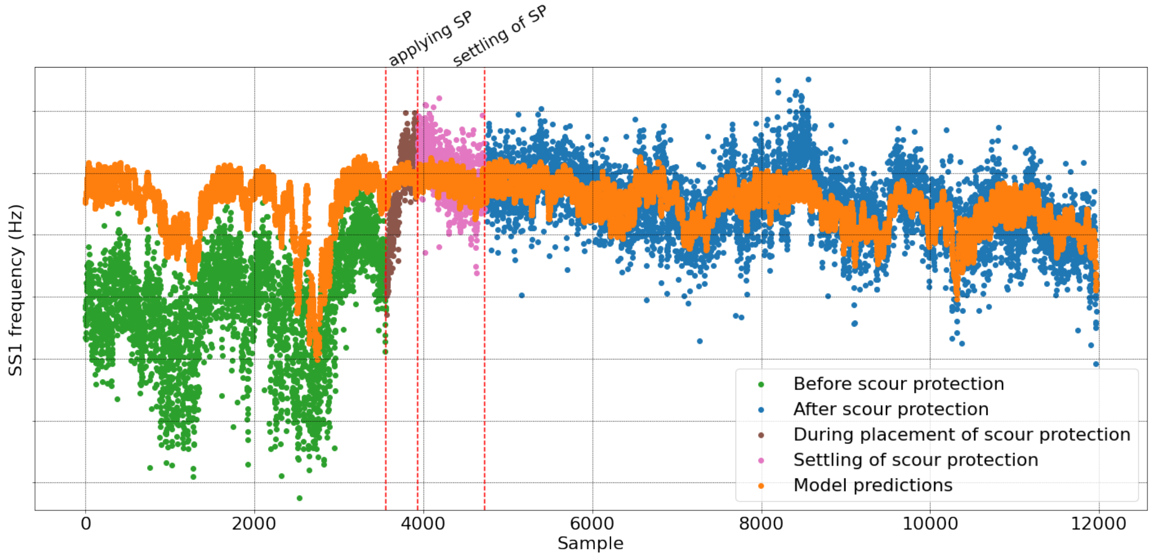

Figure 2. Tracked SS1 mode frequencies during the measurement campaign. Linear regression model predictions are shown in orange.

predict the FA1 and SS2 frequencies in the same manner as detailed above. The FA2 frequency is not investigated as it could not be tracked before the installation of the final rock armour layer. For the torsional mode, no impact of the SP was observed, and no further examination was done. Figure 3 shows the distributions of the measurements f_m and residuals f_r for SS1 and SS2. The measurement distributions are given in grey and already show a change in frequency. The residuals show a more narrow distribution both before and after SP installation, as EOV is accounted for. The method uncertainty is quantified using the standard deviation of the residuals after SP installation $\sigma_{r,after}$. The absolute change in frequency Δf_r can be computed

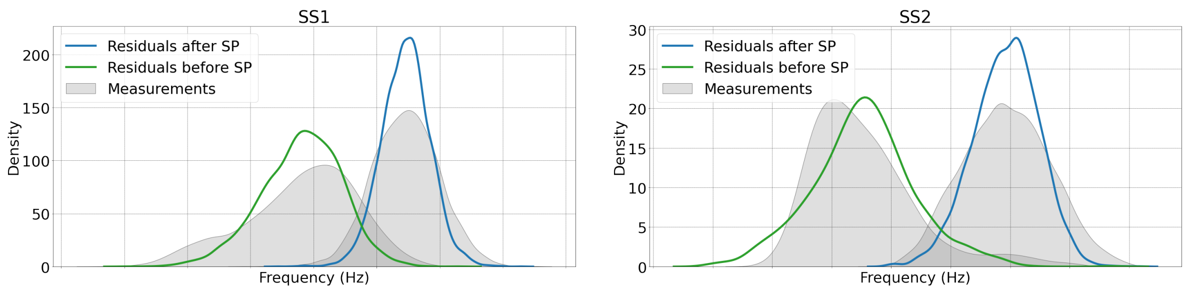

Figure 3. Distributions of the SS frequencies f_m and SS residuals f_r, before and after the installation of the rock armour layer.

by subtracting the mean residuals before from the mean residual after installation of the SP. The relative change in frequency as caused by the SP δf is calculated as a percentage, following Equation 1:

$$\delta f = \left(\frac{f_p(\mathbf{x}_{ref})}{f_p(\mathbf{x}_{ref}) - \Delta f_r} - 1 \right) * 100 \tag{1}$$

Where $f_p(\mathbf{x}_{ref})$ is the predicted frequency (with scour protection) for a reference set of environmental conditions $\mathbf{x}_{ref}$. These conditions are a wave height of 0.1m, a sea water temperature of 5°C and a tidal level of 0.5m LAT and will later be used in the models as well. The δf is given in Table 1 for the three considered modes, all values are positive in line with the observed increase in resonance frequencies once the SP was installed. The change in frequency is significant compared to the relative uncertainty $\sigma_{r,after}/f_p(\mathbf{x}_{ref})$.

Table 1. Percentile shift and uncertainty in modal frequencies after applying the additional scour protection.

	SS1	FA1	SS2
δf (%)	1.582	1.507	2.840
$\sigma_{r,after}/f_p(\mathbf{x}_{ref})$ (%)	0.367	0.496	0.650

3. Numerical model

3.1. Main assumptions

An integrated FE model was used to investigate some potential methods in which the findings could be explained. To this end, the in-house models that are used for offshore wind turbines were repurposed and modified, referencing the design documentation of the OHVS. The FE model of the complete support structure, including the monopile foundation, have been set up through the *OpenSees* simulation platform [11] using the python interpreter Openseespy [12].

Because the monopile foundation has a relatively large diameter, with an embedded L/D = 5.6 and an actual diameter within the range of 5m-10m, the PISA design method [13] was chosen to model the OHVS. the MP/TP structure is represented by a beam column model based on Timoshenko theory and the SSI is based on the four soil reaction components of the PISA model. The soil curves used to calculate the spring values were based on a geotechnical interpretation of the available in-situ and laboratory tests. The factual geotechnical data and the interpreted profile are stored in the OWI-lab meta-database [14]. The actual OHVS station was added on top of the TP as a lumped mass and connected with a rigid link to achieve a rigid kinematic coupling between the nodes. Total mass and moments of inertia were provided by the design documents. Steel properties of the structural items were set at a Young's modulus of 210GPa and a 0.3 Poisson ratio. The grout mass was included as a distributed appurtenance but any potential stiffness related to the connection is neglected with no load transfer through the grouted connection. Secondary steel equipment was also included, either as a lumped mass appurtenance (e.g. flanges) or as uniformly distributed appurtenances (e.g. boat landing) by including series of lumped mass appurtenances closely spaced. The influence of the surrounding seawater was taken into account by assuming an average tide level of 0.5m LAT with enclosed and added water mass effects (C_m=1.0) simplified as nodal lumped masses evenly distributed along the water depth. In addition, marine growth was added with a maximum thickness of 150mm and a 1.4 t/m^3 according to DNV-ST-0437. Damping was not taken into account.

3.2. Modeling approaches to include SP

To include Scour protection, two methods are proposed to model its effects. The first approach includes the scour protection as an additional layer of dense sand on top of the original soil profile, which is a common simplification and for example also used in [6]. Here, the scour protection itself is assumed to provide some lateral support to the monopile foundation. The thickness of this layer can be inferred from the bathymetric surveys conducted after SP installation. The only variable parameter will be its stiffness (G_{max} value). The second approach focuses on how the increased overburden stress, caused by the weight of the SP, affects the granular upper soil layer response in a zone of limited extend around the monopile. This is a newer approach as described in [15]. The horizontal and vertical effective stress increase below the scour protection can be calculated using elastic stress solutions. The stiffness of the granular skeleton is stress-dependent, and an increased overburden pressure will lead to an increase of the soil's small-strain shear stiffness [16]. The relation between effective stress and small strain stiffness (G_{max}) can be approximated with a power law [17]. This procedure aims to take into account the increment of small strain shear stiffness due to the increased overburden stress due to the SP weight. Past research shows that a dependence of the coefficients of the power law on the soil's compression index C_c can be identified [18]. However, C_c is not a widely available parameter for offshore geotechnical surveys, especially not in cohesionless soil. The coefficients of the power law were reformulated in terms of the soil behaviour type index I_c inferred from CPT tests. This approach first recalculates the overburden stress profile, accounting for the installed SP system. The overburden stress profile is then used to estimate the increased small shear stiffness profile. The resulting recalculated G_{max} for the upper soil layers will lead to a stiffer response of the overall structure.

4. Comparison between simulations and measurements

4.1. Initial comparison without modelled SP

The previously obtained measured values for the eigenfrequencies of the OHVS can now be compared to the initial design. To keep confidentiality, no actual values will be shown, but instead relative differences, with the design frequencies as a baseline, will be used to discuss the results as shown in figure 4. Overall, we can say that there is a noticeable discrepancy, with around 13%-13.5% higher values for first order, 7.5% higher for first torsional and 0.5% higher for second order frequencies. After Full armour had time to stabilize these discrepancies increased even further to around 15%-16%, 8% and 3%-10% respectively. The reason for this relatively big discrepancy is twofold. First, it is an older design of some years ago, predating several improvements in the design process, such as state of the art SSI (PISA). Second, it uses a model normally used for OWTs and not specifically validated for OHVS structures. Also, eigenfrequencies were not the most important design driver for the OHVS.

The integrated model shows a better agreement to the measurements, mainly due to the improved SSI. This gives higher frequencies than design, but still falls short of the measurements. An attempt was then made to better fit the integrated model by manipulating the values of the top masses of the OHVS, as these had the biggest uncertainties apart from the soil. The centre of gravity was lowered within the maximum allowed tolerance of design and the mass moment of inertia and masses were tweaked to best fit the torsional mode and the variability between FA2 and SS2. We have no actual reference values without any SP at all, only with a filter layer. Because of this, we are probably still a few percent removed from the actual in situ frequencies. But it is not our goal to have a perfect model for an OHVS, we just want to get close enough to be able to test responses of modelled scour protection. To this end the decision was made that we are close enough to do that type of analysis. In the upcoming subsections design will not be taken into account and the focus will be purely on the effect of added SP.

4.2. Global accretion SP model

This subsection will look at the viability and response of the global accretion model by performing a sensitivity study on its two most important parameters. One of these is the

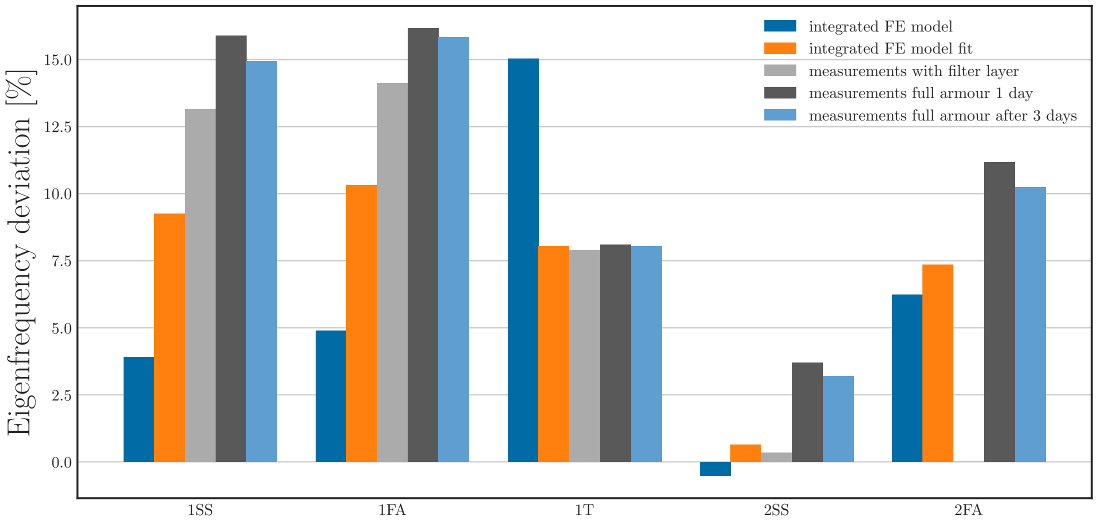

Figure 4. Both integrated FE model and measurements deviate from the as-designed frequencies. integrated FE model(dark blue)- integrated FE model with optimized parameters (orange) - measurements before SP installation (grey) - measurements directly after SP installation (black) - measurements long after SP installation (light blue).

thickness of the SP layers. Both design documents and bathymetric measurements are available, but even still, there is some uncertainty left. In practice the in situ filter layer can vary between 0.4m - 0.6m and the combined applied cushion and armour layer has a range of 0.6m - 1.4m. Together, after full installation, the SP should be anywhere between 1.1m - 2.0m with a best estimate of around 1.7m in thickness. So in this best estimate scenario, we go from 0.5m scour protection before full armour, to 1.7m scour protection after complete installation (+1.2m). Second, we have the stiffness induced by a given thickness of SP. To this end the G_{max} value of the artificially applied soil layer will be varied between 20000kPA - 120000kPa. These bounds were chosen based on comparison with actual upper soil layers in the region. It should be noted that the weight of the modelled global accretion layer also has an impact on the vertical effective stress of the underlying soil.

It is noticeable that an increase in either SP thickness or SP stifnness, lead to higher eigenfrequencies. Furthermore, this method can be used to model the effects of SP installation, as the curves cross the red line denominating the in situ measured response. However, considering the best estimate for thickness, a discrepancy is present between both first and second order (1^{st} SS = 58000kPa and 2^{nd} SS = 80000kPa) and between directions (1^{st} SS = 58000kPa and 1^{st} FA = 52000kPa). It is impossible to get a perfect fit unless the whole integrated FE model would be fine-tuned for a specific circumstance, but that is outside of the scope of this paper. With the total model as is and taking SS1 as the reference, the most optimal configuration for a global accretion layer as an approximation for SP seems to be: 1.7 m total thickness and G_{max} = 58000 kPa to derive the soil curve and spring stiffness. But due to the current unresolved modelling uncertainties, this final result should not be interpreted as a true reference value for SP stiffness. Finally it should also be noted that this methods results might vary between different structures, like for example an OWT. As such this method should only be used as an empirical formulation that can help to better fit models with their in situ structural counterpart. More tests are needed for different locations and structures to verify how robust this approach really is.

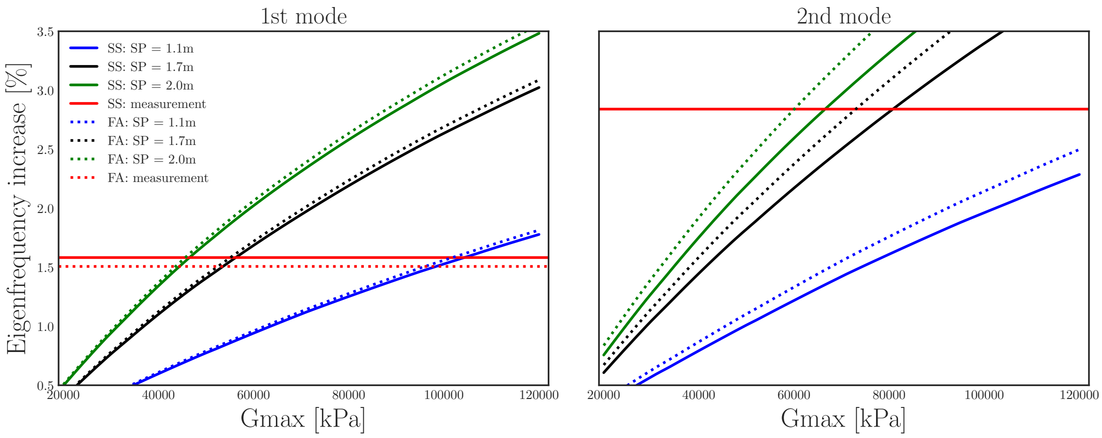

Figure 5. Increase in eigenfrequencies of the OHVS structure after the full rock armour layer has been installed on top of the filter layer, for both first and second mode, in side-side and for-aft directions.

4.3. Physics based SP model

This subsection studies the physics based model accuracy by performing a sensitivity study on its two most important parameters. Just as with the global accretion layer, thickness plays an important role. Once again a range from 1.1m - 2.0m will be used based on the bathymetric surveys, with a best estimate of 1.7m (0.5m + 1.2m full armour including cushion layer). Second is the mass density of the SP, which is derived from the submerged bulk unit weight. This ranges from 9.0kN/m^3 to 18kN/m^3, with 12.75 kN/m^3 as best estimate. For the individual pebbles/rocks this corresponds with a density of approximately 2700kg/m^3. It should be noted that the extension length of all the layers also has an effect. But this effect was negligible when staying within realistic values. As such all tests were done with the following extension lengths: 2.21D_{MP} for the filter, 2.21D_{MP} for the cushion, 1.48D_{MP} for the armour.

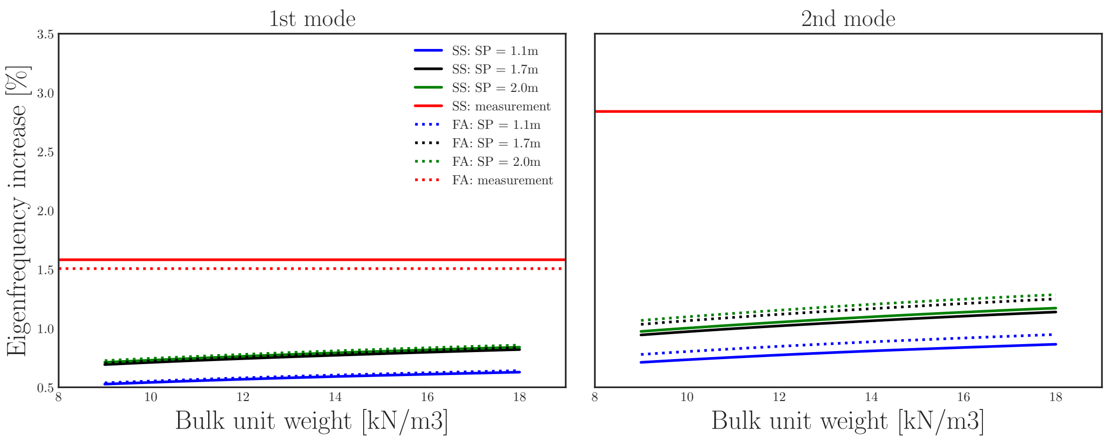

Figure 6. Increase in natural eigenfrequencies of the OHVS after the full rock armour layer has been applied on top of the filter layer, for both first and second mode, in side-side and For-aft directions.

Again, we see a proportional response for both parameters. However, the response is a lot weaker and there are diminishing returns when it comes to increasing the height of the SP. This makes sense, because as weight is being piled on, it will get harder and harder to introduce extra stiffness (increase in G_{max}) to the underlying soil layers. Also, the physics based model seems to not be able to bridge the gap needed to explain the measurements. On the positive side, this method is a conservative one and with a small sensitivity to any uncertainty concerning thickness and density of the SP.

Unlike the global accretion method, which could fit the integrated FE model to the measurements, the physics based model cannot. But its strength is its plausibility and the fact that it is rooted in a real physical phenomenon. To bridge the leftover gap with the measurements some more testing at different locations is needed. Some potential improvements are the addition of extra SSI springs in the SP layer as was done in the global accretion model, but with a stiffness that is a lot lower. It could also be that for other structures or better fine-tuned models these discrepancies will just disappear, or it might be that there is an additional effect that is not being considered at this time.

4.4. Comparison with modelled SP

Here both the global accretion and physics based model will be compared side by side against the measurements. Again, the relative increase of eigenfrequency between only the applied filter layer and the fully installed SP will be used as the reference. The dimensions will be fixed at the 1.7m thickness best estimate while the other parameters will still be varied between 20000kPa - 120000kPa and 9.0kN/m^3 - 18.0kN/m^3 to give a sense of the range of possible solutions.

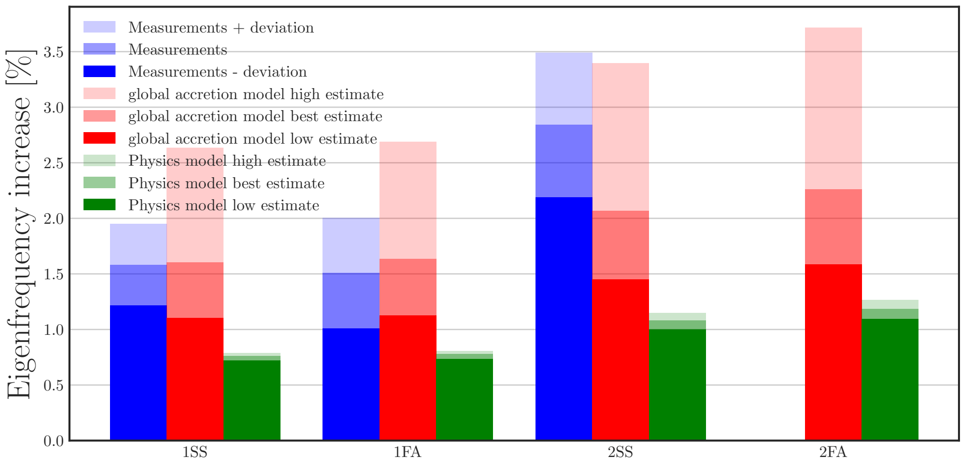

Figure 7. Comparison of eigenfrequency increase after SP installation between: measurements (blue) - Global accretion model (red) with varying stiffness - physics based model (green) with varying bulk unit weight.

As mentioned before, the global accretion model can easily be matched with any value it wants. But due to the lack of any real reference for realistic inputs, the results can vary wildly and easily under- or overshoot the target. This makes it rather volatile and only usable for model optimization of a structure that already exists. As measurement data can then be used to determine the correct input parameters. Whereas the physics based model falls short at around half of the expected increase in frequency, but it has low variability in its solutions. Also, it has input parameters that are linked to objective real-world observations.

5. Conclusion

Full scale measurements presented in this paper show that scour protection has a noticeable effect on the structure it is meant to protect. In addition to its intended anti-scouring qualities, it also stiffens the foundation. This leads to higher eigenfrequencies, which in turn lead to longer life-time expectancy or leaner design. For the discussed monopile supported OHVS this is an increase of around 1.5% for the first order and a 2.8% increase for the second order frequencies. The first torsional mode was unaffected. This result could be used to optimize future design and extend lifetime of existing structures.

Two methods to include the contribution of the SP system in the numerical model were compared against the measurements. The global accretion model can probably give a decent fit for any situation, but is volatile and the assumed input parameters cannot be justified with reference values. Although the physics-based model cannot fully explain the observed increase, the required inputs can be justified in a more straightforward manner. Looking at these results it might be best to combine both methods into one to fully describe the effect of the SP on the foundation. However, it should be noted that the modelling of the OHVS was not perfect and results may vary when we apply SP models to offshore wind turbines for which we have more accurate descriptions. For this reason, more definitive statements for best modelling practices will be kept for future work. As more tests at different locations and under different circumstances are needed to come to a final conclusion.

Acknowledgements

The authors would like to acknowledge the support of the Belgian Ministry of Economic Affairs through the ETF WINDSOIL project and The support of VLAIO through the De Blauwe Cluster SBO SOILTWIN project. As well as Parkwind for permission to use their data.

References

[1] Kallehave D, Byrne B W, LeBlanc Thilsted C and Mikkelsen K K 2015 *Phil. Trans. R. Soc.* A **373** 20140100
[2] Hald T, Mørch C, Jensen L, Bakmar C and Ahle K 2009 *Proc. of European Offshore Wind 2009 Conf.*
[3] Ma H and Chen C 2021 *Ocean Engineering* **231** 109083
[4] Askarinejad A, Wang H, Chortis G and Gavin K 2022 *Ocean Eng* **244** 110377
[5] Stuyts B, Weijtjens W, Devriendt C, Versteele H and Haute C V 2020 *4th International Symposium Frontiers in Offshore Geotechnics* (Deep Foundations Institute) p 3557
[6] Jurado C S, Stuyts B, Weijtjens W and Devriendt C 2022 *Journal of Physics: Conference Series* vol 2265 (IOP Publishing) p 032098
[7] Devriendt C, Magalhães F, Weijtjens W, De Sitter G, Cunha Á and Guillaume P 2014 *Struct Health Monit* **13** 644–659
[8] Magalhães F and Cunha Á 2011 *Mechanical systems and signal processing* **25** 1431–1450
[9] Ester M, Kriegel H P, Sander J, Xu X *et al.* 1996 *kdd* vol 96 pp 226–231
[10] Weijtjens W, Verbelen T, De Sitter G and Devriendt C 2016 *Struct Health Monit* **15** 389–402
[11] McKenna F 2011 *Comput. Sci. Eng.* **13** 58–66
[12] Zhu M, McKenna F and Scott M H 2018 *SoftwareX* **7** 6–11
[13] Byrne B W, Houlsby G T, Burd H J, Gavin K G, Igoe D J, Jardine R J, Martin C M, McAdam R A, Potts D M, Taborda D M *et al.* 2020 *Géotechnique* **70** 1030–1047
[14] Stuyts B, Weijtjens W and Devriendt C 2022 *Acta Geotech* 1–15
[15] Stuyts B 2023 *Improved Soil-structure interaction for offshore monopiles based on in-situ monitoring data* Phd thesis Free university of Brussels Brussels
[16] Lyu C, Park J and Santamarina J C 2021 *Journal of Geotechnical and Geoenvironmental Engineering* **147** 1–15
[17] LeBlanc C, Houlsby G and Byrne B 2010 *Géotechnique* **60** 79–90
[18] Cha M, Santamarina J C, Kim H S and Cho G C 2014 *Journal of Geotechnical and Geoenvironmental Engineering* **140** 06014011